

## 3-2 Cesium Primary Frequency Standard

### 3-2-1 Optically Pumped Cesium Primary Frequency Standard

FUKUDA Kyoya, HASEGAWA Atsushi, ITO Hiroyuki, KUMAGAI Motohiro, KOTAKE Noboru, KAJITA Masatoshi, HOSOKAWA Mizuhiko, and MORIKAWA Takao

Communications Research Laboratory (CRL) has developed an optically pumped primary frequency standard named CRL-O1 in cooperation with the National Institute of Standards and Technology (NIST). The accuracy of CRL-O1 has been evaluated and reports have been sent to the BIPM. In these reports, the two type uncertainties, that is type A and B involved in the frequency shift, are estimated. The total combined uncertainty is less than  $6 \times 10^{-15}$  which normalized by the frequency of Cs clock transition. The results of the evaluation were published in the Circular-T. The evaluated frequency of CRL-O1 is in good agreement with that of other primary frequency standards.

#### *Keywords*

Optically pumped primary frequency standard, CRL-O1, Accuracy evaluation, Frequency shift, Uncertainty

#### 1 Introduction

The center frequency of an eigenspectrum of an atom, a molecule, or an ion is as fixed and unchangeable as the basic physical constants. Based on this principle, an atomic frequency standard consists of an oscillator that uses a high-resolution spectroscopic technique to obtain a highly accurate spectrum.

The second is currently defined in terms of frequency as "equal to 9,192,631,770 periods of the radiation corresponding to the transition between the two hyperfine levels of the ground state of an atom of Cs<sup>133</sup>," as stipulated at the CGPM (General Conference on Weights and Measures) in 1967. Under this definition, it is assumed that the atom is in an ideal state; i.e., free from any perturbations. However, in order to measure a physical quantity, it is necessary to add a certain perturbation to an object and to observe the response. Conse-

quently, a measured frequency will deviate from the defined value due to various physical effects. Therefore, if the factors and extent of the measurement-induced shift in frequency are not known, measurement results will not be accurate in terms of the defined units. A primary frequency standard consists of equipment that can evaluate and adjust for this shift, thus ensuring accurate time measurement based on the standard frequency [1][2]. Accuracy is therefore determined by the degree to which uncertainty induced by factors affecting the shift may be measured and corrected. Accordingly, continuous operation of the standard is challenging, due to the complexity of the evaluation of these factors.

Almost all of the various global standard times, including Japan Standard Time—generated and maintained by the Communications Research Laboratory (CRL)—are based on commercial cesium atomic clocks capable of

continuous operation (secondary frequency standards). Although these atomic clocks provide excellent long-term stability, the devices themselves cannot measure frequency shift factors on their own. Therefore, these clocks must be evaluated and corrected using exceptionally accurate, absolute primary frequency standards. Only seven highly accurate primary frequency standards, located in four countries, are currently used to calibrate the international coordinated universal time (UTC) standard. The CRL-O1 optically pumped primary frequency standard, developed through cooperation between the CRL and the U.S. National Institute of Standards and Technology (NIST) is one such standard. This particular device is capable of defining the second with an uncertainty of  $6 \times 10^{-15}$ [3][4].

## 2 Optically pumped primary frequency standard

Fig.1 shows a basic schematic diagram of the CRL-O1 optically pumped Cs atom primary frequency standard. The CRL-O1 features numerous components, including a cylinder beam tube, a vacuum pump, a laser light source, a microwave synthesizer, and a measurement and control computer unit. The total system measures 1.2 m in height, 1 m in depth, and 3.2 m in width. The beam tube has a symmetrical appearance, as shown in Fig.1.

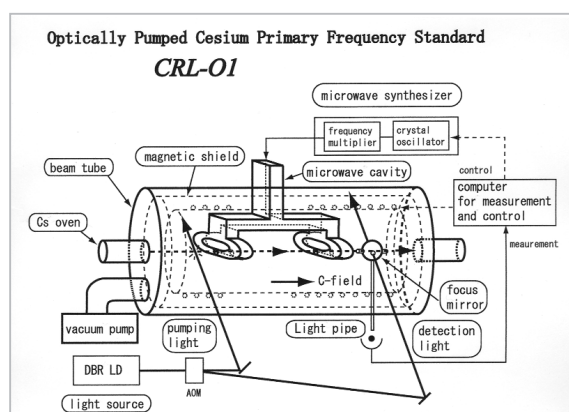


**Fig. 1** Schematic diagram of optically pumped Cs atom primary frequency standard

Cs ovens are installed at both ends of the beam tube. Cs atoms are heated to about  $100^\circ\text{C}$  in these ovens, and are made to enter the beam tube in the form of a beam after passing through a narrow tube (a collimator, with a diameter of 3 mm and a length of 50 mm). To absorb excessive Cs atoms, a cylinder of carbon graphite is placed between the collimator and the beam tube. The obtained atomic beam irradiates approximately  $10^8$  atoms/sec at the site of detection.

The Cs atom may be in one of two ground states: one in which the total angular momentum quantum number  $F$  is 3, or one in which the quantum number is 4. Immediately following emission from the ovens, these two states of atoms are present in nearly equal amounts in the atomic beam, but by the optical pumping effect of the laser light (optical pumping light), all the atoms are driven into the  $F=3$  atomic energy state. If a microwave is applied twice in succession through the Ramsey cavity to the beam of atoms that have been driven completely to the  $F=3$  state, Ramsey resonance will take place. In this way, the probability of the beam atoms being either in the  $F=3$  state or the  $F=4$  state after passing through the cavity becomes highly dependent upon microwave frequency. A standard frequency measures the number of atoms in the  $F=4$  state in the atomic beam and determines the microwave frequency at which the transition to the  $F=4$  state occurs most efficiently (i.e., the frequency of transition between the hyperfine levels). The obtained line width of the spectrum (Ramsey spectrum) depends on the time of flight of the atomic beam between the two interaction regions.

Since the quality of the microwave cavity is directly related to numerous factors contributing to frequency shift, this is the most important characteristic of the standard. Since microwave phase difference between the interaction regions in two locations causes frequency shift, the cavity must be as symmetrical as possible in order to minimize such phase difference. Moreover, if the resonance frequency of the cavity deviates from the reso-

nance frequency of the atom, a frequency shift will be produced (referred to as a cavity pulling shift); therefore, it is also necessary to minimize this frequency difference. Furthermore, since frequency shift is also caused by leakage of the microwave from the cavity and from the microwave supply component, extra care is required in the manufacture of these parts. In the design of the cavity of the CRL-O1, close attention was paid to such frequency shift factors. The cavity uses a U-shaped rectangular wave guide in which an H-plane is used in  $TE_{10}$  mode. The interaction region is divided by a drift region 1.53 m in length into two interaction regions, each 23 mm in length. We adopted a DeMarchi cavity, featuring a ring-type structure[5], substantially reducing frequency shift arising from non-uniform phase distribution inside the cavity in the interaction regions. The cavity has a hole 3 mm in diameter through which the atomic beam passes. The loaded Q value of the cavity is about 400.

Since our standard uses an H-plane cavity, the static magnetic field (C-field) used to produce Zeeman splitting is parallel to the atomic beam. A solenoid coil to generate the C-field is wound around an aluminum bobbin and covers nearly the entire beam tube. This coil is covered with a three-fold magnetic shield. Magnetic shielding factors perpendicular to and parallel to the atomic beam direction are on the order of  $10^6$  and  $10^3$ , respectively. In order to supplement reduced the magnetic shielding factor in the parallel direction and also to minimize the effects of geomagnetism, the beam tube is positioned in an east-west orientation. Moreover, the C-field is actively controlled to ensure generation of a constant magnetic field.

An ion pump is used to regulate the beam tube to maintain a degree of vacuum equal to or less than  $10^{-8}$  Torr (pumping speed of 20 l/s). A constant temperature (approximately  $37^\circ\text{C}$ ) is maintained using a nonmagnetic heater and thermal insulation.

A microwave of 9.2 GHz corresponding to the frequency of clock transition is obtained

by multiplying and synthesizing outputs of voltage control crystal oscillators (VCXO) of 5 MHz, 100 MHz, 10.7 MHz. All the VCXOs are phase locked to a hydrogen maser acting as a standard oscillator and are linked to the original signal for Japan Standard Time, designated as "UTC (CRL)." The 10.7-MHz VCXO is phase locked to a DDS (Direct Digital Synthesizer) controlled by a PC, and is capable of sweeping a range of about 360 kHz around a center frequency of 9.2 GHz. Microwave intensity can be set to an arbitrary intensity with reduced fluctuation using a power servo circuit; this intensity then may be controlled by the PC. In order to determine the center of the atomic resonance line, slowly changing square-wave modulation is applied.

A 20-mW DBR laser (its frequency stabilized relative to a Cs absorption line using the FM sideband method) is used to excite the atom. The laser light is divided into two beams: one for optical pumping, and the other for detection. In our standard, the optical pumping light and the detection light are tuned to the transition from the  $F=4$  ground state to the  $F'=3$  excited state as well as to the transition from the  $F=4$  state to the  $F'=5$  excited state. The laser light is of linear polarization and is irradiated to the atom from a direction perpendicular to the direction of travel. The optical pumping light that passes through the beam tube is then reflected by a double-refraction prism and is again irradiated to the atomic beam. This reflected light is polarized perpendicular to the incident light, thus increasing the efficiency of optical pumping. By this method, the atom is transformed from the  $F=4$  energy state to the  $F=3$  state at almost 100% efficiency, without the atomic transition to the dark state normally generated by laser-light irradiation. A spherical mirror and an ellipsoidal mirror are combined to form a mirror for collecting fluorescence from the atoms that have interfered with the microwave, and the collected light is extracted to the outside of the vacuum chamber by a light-pipe. The extracted fluorescence is converted to an electrical signal using a high-sensitivity optical detector

and an operational amplifier, and this signal is then sent to the measurement and control computer through an AD converter.

### 3 Frequency shift and uncertainty

When the frequency of the clock transition of the cesium atom is measured, various exterior perturbations are introduced; as a result, the measured frequency differs from the original frequency of the cesium atom. By definition, however, the frequency of the clock transition between the ground states of the cesium atom must be determined in the absence of any such perturbations. Therefore, in order to determine the value for definition experimentally, the extent of the shift due to perturbation (referred to hereinafter as the frequency shift quantity) must be estimated and the measurement value adjusted accordingly. The uncertainty of this estimation is also an important parameter in the application of the primary frequency standard; the process of estimation and the associated uncertainty will be discussed separately below[6][7].

Improving the accuracy of these estimates continues to form a significant focus of research. According to the guidelines of the International Committee of Weights and Measures (BIPM = Bureau International des Poids et Mesures)[8], uncertainty can be divided into that induced by statistical variation (type A) and that induced by systematic deviation in measured values (type B). From here through section 3.6 below we will describe type B uncertainty (type A uncertainty will be discussed in section 3.8). All values listed below are expressed in the order of magnitude of  $10^{-15}$ , and are obtained using the clock transition frequency to normalize the frequency width corresponding to the estimated uncertainty.

#### 3.1 Second-order Doppler shift

Since the microwave is applied perpendicular to the travelling direction of the atom, it is not necessary to consider the first-order Doppler shift. However, according to the theory of relativity, time viewed from the coordi-

nate system of a stationary observer differs from time within the coordinate system of the traveling atom (atomic eigentime). The frequency shift quantity in this case is given by

$$\delta\nu_D = -\frac{1}{2} \frac{V^2}{c^2} \nu_{Cs} \quad (1)$$

Here,  $V$  denotes the velocity of an atom cluster,  $c$  the velocity of light, and  $\nu_{Cs}$  the clock transition frequency of the cesium atom, 9,192,631,770 Hz. This equation is for an atom cluster having a single velocity. Since generally atom clusters feature a distribution of velocities, however, the weighted integral of the value determined by this equation will correspond to the frequency shift quantity for such an atom cluster. In this case, we must determine the velocity distribution; this is done by measuring Ramsey signals (using several microwaves of different intensities) and then performing Fourier transformation on these signals[9].

Type B uncertainty in the second-order Doppler shift depends on the accuracy of the determination of velocity distribution. The statistical uncertainty accompanying the Fourier transformation was 0.6. The uncertainty arising from potential instability of the microwave power servo was 1.8. Therefore, overall uncertainty of the second-order Doppler shift was estimated to be 2.

#### 3.2 Quadratic Zeeman shift

Zeeman shift refers to a change in the resonance energy of an atom resulting from application of an external magnetic field. The clock transition of the cesium atom is the transition from a ground state in which  $F=4$  and  $m_F=0$  to one in which  $F=3$  and  $m_F=0$  (hereinafter referred to as a "0-0 transition" referring to the  $m_F$  values of the two ground states), where  $F$  denotes the total angular momentum quantum number, and  $m_F$  denotes the magnetic quantum number. In order to observe the frequency of this transition, a C-field is applied to the microwave cavity of the standard in such a way as to prevent transitions between other Zeeman sub-levels. The shift in the 0-0

transition frequency due to this magnetic field is the quadratic Zeeman shift. Here the shift quantity is expressed by the following equation.

$$\delta\nu_{QZ} = 8\nu_z^2 / \nu_{Cs} \quad (2)$$

Here,  $\nu_z$  denotes the Zeeman Frequency, or the difference between the frequency of the 0-0 transition and that of the 1-1 transition. The uncertainty associated with this shift quantity depends on the frequency stability of the servo circuit used to control the C-field. Since the accuracy of the determination of the Zeeman frequency in this circuit is 0.01 Hz or lower, the uncertainty is 0.2 or less.

### 3.3 Cavity pulling shift

This shift is caused by the difference (detuning) between the resonance frequency of the microwave cavity and the atomic resonance frequency. This phenomenon occurs when the resonance frequency of the cavity deviates from that of the atom, resulting in deformation of the atomic resonance line and in an apparent shift in the frequency of the resonance peak. The shift quantity in this case can be expressed by the following equation.

$$\delta\nu_c = \frac{\partial P / \partial b}{\partial P / \partial \lambda} \times \frac{db}{d\lambda} \times \omega_m \quad (3)$$

Here,  $\lambda$  denotes detuning of the microwave,  $P$  represents transition probability,  $\omega_m$  is the amplitude of modulation, and  $b$  is the Rabi frequency. In this case, the quantity  $db/d\lambda$  is dependent solely on the detuning between the cavity and the line width<sup>[10]</sup>.

Since the cavity of the CRL-O1 is constructed with great care, this shift is extremely small. System stability when the frequency was stabilized to the center of the Rabi resonance frequency was found to be approximately  $2 \times 10^{-11}$  for a period of 100 s. By extrapolating this to a value corresponding to a full day of measurement (86,400 sec) and also taking into account the frequency shift due to Ramsey resonance (this shift is approximately three orders of magnitude smaller than that of Rabi resonance), type B uncertainty

was estimated at 0.6.

### 3.4 End-to-end cavity phase shift

This shift is peculiar to a Ramsey type cavity with two resonance regions. If the phase of the microwave differs between the occurrence of the first and second resonance, the peak of the Ramsey signal is shifted. This shift can be reversed and thus corrected by reversing the direction of the atom beam used in measurement. However, if trajectories of the beams at both resonances do not perfectly coincide, distributed cavity phase shift occurs, limiting the accuracy of the correction. However, since we have adopted a ring-type cavity, the shift quantity is structurally minimized. This shift quantity can be expressed by the following equation.

$$\delta\nu_E = \phi E \quad (4)$$

Here,  $\phi$  denotes the phase difference between the cavities; this value is determined from measurement data.  $E$  denotes the time required for the cesium atom to pass through the two cavities; this value is related to the velocity distribution of the atom cluster. The uncertainty of the resonance frequency in this case can be expressed by

$$\delta\nu_E = \left( \frac{\partial E'}{E'} - \frac{\partial E}{E} \right) \frac{EE'}{E + E'} \phi \quad (5)$$

Here,  $E$  and  $E'$  denote different values of  $E$  in accordance with the different directions of the atomic beam. The equation shows that the uncertainty is dependent on the accuracy of the determination of phase difference and of the velocity distribution. In this case we estimated uncertainty to be 0.2 or less.

### 3.5 Blackbody radiation shift

This shift originates from pumping of a non-resonant atom by background blackbody radiation. This shift can be interpreted as an AC Stark effect, with a theoretical equation given by

$$\delta\nu_B = -1.711 \times 10^{-14} [(T + 273.15) / 300]^4 \nu_{Cs}, \quad (6)$$

In this case, the measurement error of the temperature inside the standard determines the uncertainty of the frequency. Roughly estimating the temperature-induced measurement error to be 2°C, we assumed an uncertainty value of 0.5.

### 3.6 Gravitational shift

This shift is induced by the earth's gravitational field. Since the frequency of TAI is currently defined as a value on an assumed geoid surface, measured frequency must be corrected accordingly. A theoretical equation for this correction is given by

$$\delta\nu_g = (gh/c^2)\nu_{Cs} \quad (7)$$

where  $h$  denotes height from the geoid surface. Error in this measurement of height represents an additional factor determining uncertainty. Experimental results indicated that such error was on the order of several tens of centimeters. This corresponds to uncertainty of 0.1 or less.

### 3.7 Other frequency shifts

Factors other than those described above also contribute to frequency shift, some of which will be discussed later. However, the effects of most such factors were deemed sufficiently small in the present evaluation of the accuracy of the CRL-O1; only potentially non-negligible factors were considered.

#### (1) Light shift

This is a phenomenon in which the atom absorbs the laser light used for optical pumping or detection and emits fluorescence to the beam axis, resulting in a change in the energy of the atom due to the optical Stark effect.

#### (2) Distributed cavity phase shift

This shift is generated by variation in the phase distribution of the microwave in the hole through which the atomic beam in the microwave cavity passes. This shift also affects the measurement of the end-to-end cavity phase shift described above. This shift becomes significant with conventional cavity structures that rely on reflection at the waveguide terminations. The cavity we use fea-

tures ring-shaped terminations, as shown in Fig.1, to minimize this shift.

#### (3) Collisional shift

This frequency shift is generated by the collisions between the atoms.

In reality, if such collision were to occur, causing the phase of the ground state to vary during the atom's trajectory, the Ramsey signal itself would disappear; therefore, this shift would not result in phase variation.

It is conceivable that factors other than the three discussed above may cause frequency shift; however, it is presumed that the total extent of such shift—including shift induced by the three factors discussed above—will be small. The major factors contributing to frequency shift remain those discussed in sections 3.1 through 3.6. We should note, however, that this assessment is considered to apply to measurement using the optically pumped primary frequency standard; with atomic fountain primary frequency standards (expected to be used widely in the future) other factors may emerge for evaluation. Furthermore, as measurement accuracy is improved, even more factors will come to light. In the current case, shift caused by unidentified factors deemed negligible in terms of our equipment (uncorrected biases) was assumed to be 0, with uncertainty (type B) estimated as 3.2 or less.

### 3.8 Type A uncertainty

In the evaluation of accuracy, measurement is performed for ten days (one day for one data point) to determine the frequency difference between the hydrogen maser and the CRL-O1. We arrive at an accuracy value by subtracting all of the above-mentioned shift quantities from daily measured values. Since each daily measurement value collected features dispersion, the standard deviation of the daily measurement data is calculated and divided by the square root of the degree of freedom of measurement to obtain a value for type A uncertainty.

In the evaluation of the CRL-O1, accuracy can be seen in terms of (a) the stability of the

CRL-O1 itself, (b) the stability of a reference, and (c) other stabilities. The stability of actual measurement is the sum of these stability values, which is given by the equations (8), (9).

$$\sigma_r^2 = \frac{1}{n-1} \sum_{i=1}^n (R_i - M)^2, \quad (8)$$

and

$$M = \frac{1}{n} \sum_{i=1}^n R_i \quad (9)$$

Here,  $n$  denotes the number of frequency measurements and  $R_i$  denotes the measured value from which the frequency shift quantities (determined for the respective measurements) were subtracted. We used a Russian hydrogen maser (Oscilloquartz SA, CH1-75) as a reference; the stability of this reference, evaluated by Allan variance, was as follows:  $2 \times 10^{-13}$  for measurement with a sampling time of 1 sec,  $2 \times 10^{-15}$  for a measurement of 10,000 sec, and  $1 \times 10^{-14}$  for a measurement of 10 days.

On the other hand, the stability of the CRL-O1 itself is always evaluated in terms of a single second with reference to the hydrogen maser, and one-day stability is estimated based on this value, which is given by the following equation.

$$\sigma_s^2 = \frac{1}{n-1} \sum_{i=1}^n S_i^2, \quad (10)$$

Here,  $S_i$  denotes the estimated stability for each measurement. The value obtained from this evaluation must be considered as a theoretical minimum value of type A uncertainty. However, in a finite data set obtained over the course of 10 days of measurement,  $\sigma_r$  may occasionally be less than this minimum value. In such cases, we would use not  $\sigma_r$  but  $\sigma_s$  for the evaluation of type A uncertainty. Therefore, type A uncertainty  $u_A$  is expressed by the following equation.

$$u_A = \frac{\sigma_j}{\sqrt{n}} \quad (11)$$

However, if  $\sigma_r > \sigma_s$ , then  $\sigma_j = \sigma_r$ , and if  $\sigma_r < \sigma_s$ , then  $\sigma_j = \sigma_s$ .

### 3.9 Total combined uncertainty

The main uncertainties mentioned in our report to the BIPM consist of the type A and type B uncertainties described above. The square root of the sum of the squares of the above-mentioned uncertainties (both type A and type B) plus all other uncertainties—such as the uncertainty of the link between the UTC (CRL) (the time system managed by the CRL) and the hydrogen maser, the uncertainty of the link between the UTC (CRL) and TAI (International Atomic Time)—forms a total combined uncertainty that is publicized in the Circular T.

## 4 Bulletin report to BIPM

These measurement results are summarized as follows, and together comprise the accuracy evaluation of the CRL-O1 as reported to BIPM.

(1) Frequency difference between the definition value and the UTC (CRL) value, determined by subtracting the frequency shift quantities described in sections 3.1 through 3.6 from the measured frequency value

(2) Frequency shift quantities, their type B uncertainties and type A uncertainties, and the uncertainty of the link between CRL-O1 and UTC (CRL)

(3) As auxiliary data, the difference between the frequency determined using the hydrogen maser and that determined using UTC (CRL)

A portion of the latest report we have submitted is shown in Table 1. Each frequency shift quantity is calculated by the above-mentioned theoretical equation using actual measurement values. For type A uncertainty, a value of  $5 \times 10^{-15}$  was obtained. This is one of the better accuracy values obtained over 10 days of evaluation results.

In Table 1, type B uncertainty of the end-to-end cavity phase shift is 0.8. The uncertainty values described in section 3.4 reflect results obtained based on a detailed evaluation conducted after issuance of this report.

Fig.2 shows a plot of the difference

**Table 1** Results of accuracy evaluation of the CRL-O1

Frequency Biases and Their type B Uncertainty.  
(Units are fractional frequency  $\times 10^{-15}$ )

Physical Effect	Bias	type B Uncertainty
Second-order Doppler	-258.5	2
West-to-East	-290.2	
East-to-West		
Second-order Zeeman	+152,797.1	0.2
Cavity pulling	0	0.6
Cavity phase (end-to-end)	135.6	0.8
West-to-East	-143.3	
East-to-West		
Blackbody	-19.5	0.5
Gravitation	8.2	0.1
Uncorrected biases	0	3.2
Total type B uncertainty		$\leq 3.9$

The frequency difference between UTC(CRL) and H maser which we used for evaluation was  $Y_{(UTC(CRL)-H\ maser)} = +222.4 \times 10^{-15}$ .

The measured frequency between CRL-O1 and H maser was  $Y_{(CRL-O1-H\ maser)} = +208.5 \times 10^{-15}$ .

After the correction of blackbody and gravitational shift, we obtained the value of  $Y_{(CRL-O1-H\ maser)} = +219.8 \times 10^{-15}$ .

The final value of the frequency between the CRL-O1 and the UTC(CRL) was  $Y_{(CRL-O1-UTC(CRL))} = -2.6 \times 10^{-15}$ .

Corrected Value	type A Uncertainty
-2.6	5

Type A uncertainty of link between CRL-O1 and UTC(CRL) : 0.8

between the measured frequencies of CRL-O1 optically pumped primary frequency standards, those of other research organizations, and International Atomic Time (TAI); these differences are shown on the vertical axis, with year/month/day of measurement (in units of modified Julian day: MJD) on the horizontal axis. In the figure, data denoted by the Circular T is a value based on multiple data items for all of the primary frequency standards, including the magnetic-selection type standard and the atomic fountain type standard.

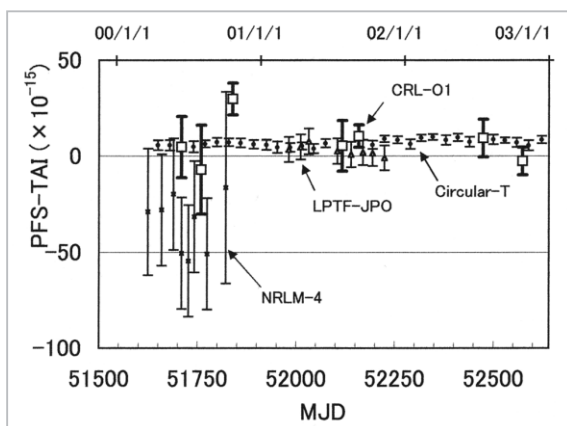


**Fig.2** Comparison of measurement results of the optically pumped primary frequency standards of CRL-O1 and those of other research organizations

Based on the diagram, we can conclude that the CRL-O1 is the most accurate device among all current optically pumped primary standards for definition of the second. However, in recent years, the advent of the atomic fountain type primary frequency standard has considerably reduced the uncertainty associated with the definition process. The uncertainty of the PTB's atomic fountain type standard (the PTB-CSF1) is approximately 2.0 to 2.5. The NIST atomic fountain type standard (NIST-F1) has reported uncertainty of about 1.5 to 2.0. The CRL-O1 primarily features type A uncertainty. With increasing amounts of measurement data type A uncertainty can be further reduced. However, since the frequency drift of the hydrogen maser currently used as the reference in the measurement period affects the shift quantity of the measured frequency, some correction will be required. The calculated average value of the frequency differences between the multiple commercial Cs clocks and the UTC official announcement value becomes as small as  $10 \times 10^{-15}$  to  $20 \times 10^{-15}$  in terms of variation width; therefore, this average can be used to correct frequency variation of the hydrogen maser for the period of evaluation. In this case we can perform correction based on a drift trend that is predicted based on past frequency variation data. Then, for the evaluation of reference standard accuracy, a reference signal may be used that has been adjusted according to the predicted trend using a frequency offset generator.

## 5 Conclusions

In collaboration with the NIST, the CRL has developed the CRL-O1 optically pumped primary frequency standard. We have reported on the results of accuracy evaluations conducted since April 2000, contributing in the process to the high accuracy of International Atomic Time. The accuracy evaluation results for the CRL-O1 agree well with BIPM values. A system for minimizing the frequency drift of the hydrogen maser used as the reference in the accuracy evaluation is now under con-



struction, and we believe that type A uncertainty can be further reduced through long-term measurements. We are currently preparing a paper dealing with the CRL-O1 accuracy evaluation; the paper is intended to report on the details of the device, measurement results, a method of evaluating shift quantities and uncertainties, and more.[11].

## Acknowledgments

We are thankful to Dr. R. Drullinger and members of the NIST Time and Frequency Division, who supported us with helpful discussions and opinions in the course of the development of the CRL-O1 and in the corresponding evaluations of accuracy.

## Appendix

Here we will describe Ramsey resonance. In a Ramsey system, atoms and microwaves interact in two separate regions, and a resonance signal is observed. The two interaction regions have the same structure. There are two types of cavities: with one, the direction of travel of the atomic beam is perpendicular to the direction of the microwave magnetic field in the interaction regions (E-bend type); with the other, the direction of travel of the atomic beam is parallel to the direction of the microwave magnetic field (H-bend type). An H-bend type cavity is used in the CRL-O1.

Analysis is straightforward with a single interaction region; when a weak C-field is applied to the atom and multiple Zeeman sub-levels in the ground state can be sufficiently separated, the atom can be treated using the two-level model. The resonance of the atom and the microwave in a single interaction region is referred to as Rabi resonance. The resonance-spectrum line width is inversely proportional to the period of interaction between the atom and the microwave.

Analysis is complex, however, with two interaction regions. In this case two interaction regions each of a length  $l$  are separated by a space of length  $L$ . No microwave is present

in the space between the two regions; this is referred to as the drift space. Consider a case in which the static magnetic field of the drift space is equal to the C-field of the interaction regions, and the atomic beam of a single velocity  $v$  passes through the two interaction regions and the drift space. The resonance between the atom and the microwave at this moment is referred to as the Ramsey resonance, and its transition probability  $P_2$  is given by the following equation[12].

$$P_2(\tau) = \frac{4b^2}{\Omega^2} \sin^2 \frac{1}{2} \Omega \tau \left( \cos \frac{1}{2} \Omega \tau \cos \frac{1}{2} \Omega_0 T - \frac{\Omega_0}{\Omega} \sin \frac{1}{2} \Omega \tau \sin \frac{1}{2} \Omega_0 T \right)^2 \quad (\text{A.1})$$

where  $b = \mu_B B / \eta$ ,  $\mu_B$ : Bohr magneton,  $B$ : microwave magnetic-field strength,  $\eta$ : Plank constant,  $\Omega = \sqrt{b^2 + \Omega_0^2}$ ,  $\Omega_0 = \omega - \omega_0$ ,  $\omega$ : microwave frequency,  $\omega_0$ : resonance frequency of the atom,  $T = L/v$ : time required for the atomic beam to pass through the drift space,  $\tau = l/v$ : time required for the atomic beam to pass through the single interaction region.

The transition probability  $P_2(\tau)$  is dependent on the microwave intensity. It reaches local maximum at  $\Omega_0 = 0$ , namely  $\omega = \omega_0$ , and takes the highest value of 1 at  $b\tau = \pi/2$ . The equation (A.1) indicates that with increasing  $T$ , the transition probability becomes more sensitive to the microwave frequency  $\omega$  and a narrower resonance spectrum can be obtained.

The spectrum component generated by each Rabi resonance in the two interaction regions is called the Rabi pedestal, and is expressed by the following equation.

$$P_3(\tau) = \frac{b^2}{2\Omega^2} \left( \sin^2 \Omega \tau + \frac{\Omega_0^2}{\Omega^2} (1 - \cos \Omega \tau)^2 \right) \quad (\text{A.2})$$

This is obtained by averaging the high-frequency component of the transition probability of the Ramsey resonance. The observed spectrum becomes a superposition of the Rabi pedestal  $P_3$  and the Ramsey resonance spectrum  $P_2$ . In the foregoing example, only the case in which the atomic beam has a single velocity  $v$  was considered; however, an actual atomic beam features velocity distribution.

The most probable velocity of the atomic beam used for the optically pumped standard is approximately 260 m/s, and the full width at half maximum of the velocity distribution is approximately 120 m/s. Therefore, the observed resonance signal becomes a superposition of resonance signals of atoms with various velocities, and consequently distinct maximum and minimum points in the Ramsey resonance (Ramsey fringe) are observed only in the near vicinity of the resonance frequency of the atom.

In the atomic fountain type frequency standard, the atomic speed is minimized by laser cooling technology. The atomic beam used for microwave resonance has an average velocity of approximately 1 m/s and the width of the velocity distribution is a few cm/s or less. Therefore, as shown in the present section **3-2-2**, "Atomic fountain type frequency standard," a spectrum narrower than that of the optically pumped frequency standard is obtained and the Ramsey fringe is observed over the entire Rabi pedestal.

## References

- 1 S. Urabe, J. Umezu, M. Ishizu, and R. Hayashi, "New Atomic Frequency Standards", Journal of The Radio Research Laboratory, Vol.29, No.149, pp.141-159, 1983.
- 2 Y Koga, S. Ohsima, Y. Nakadan, and T. Ikegami, "Construction of an optically pumped cesium beam frequency standard", Bulletin of NRLM, Vol.38, No.1, pp49-56, 1989. ( in Japanese)
- 3 A. Hasegawa, K. Fukuda, N. Kotake, M. Kajita, T. Morikawa, W. D. Lee, C. Nelson, D. A. Jennings, L. O. Mullen, J. H. Shirley, and R. Drullinger, "An Improved Optically-pumped Primary Frequency Standard", Proc. of Frequency Control Symposium98, pp. 61-63, 1998.
- 4 A. Hasegawa, K. Fukuda, N. Kotake, M. Kajita, T. Morikawa, W. D. Lee, C. Nelson, D. A. Jennings, L. O. Mullen, J. H. Shirley, and R. Drullinger, "CRL-NIST Joint Development of An Improved Optically pumped Primary Frequency Standard ", Proc. Conf. on Precision Electromagnetic Measurements, pp.177-178, 1998.
- 5 A. DeMarchi, O. Francescangeli, and G. P. Bava, "Dimensional Sensitivity of End-to-End Phase Difference in Ring Terminated Ramsey Cavities", IEEE Trans. Instrum. Meas., Vol.42, No.2, pp.448-452, 1993.
- 6 W. D. Lee, J. H. Shirley, J. P. Lowe, and R. E. Drullinger, "The Accuracy Evaluation of NIST-7", IEEE Trans. Instrum. Meas., Vol.44, No.2, pp.120-123, 1995.
- 7 J. H. Shirley, D. W. Lee, and R. E. Drullinger, "Accuracy evaluation of the primary frequency standard NIST-7", Metrologia Vol.38, pp.427-458, 2001.
- 8 "Guide to the expression of Uncertainty in Measurement", published by International Organization for Standardization.
- 9 J. H. Shirley: "Velocity distribution calculated from the Fourier transforms of Ramsey lineshapes", IEEE, Trans. Instrum. Meas. Vol. 46, No.2 pp.117-121, 1997.
- 10 J. H. Shirley, D. W. Lee, G. D. Rovera, and R. E. Drullinger, "Rabi Pedestal Shifts as a Diagnostic Tool in Primary Frequency Standards", IEEE, Trans. Instrum. Meas. Vol. 44, No.2 pp.136-139, 1995.
- 11 A. Hasegawa, K. Fukuda, M. Kajita, H. Ito, M. Kumagai, M. Mizuhiko, N. Kotake, and T. Morikawa, in preparation.
- 12 J. Vanier and C. Audoin, "The Quantum Physics of Atomic Frequency Standards", Adam Hilger, Bristol and Philadelphia, 1989.



**FUKUDA Kyoya**

*Senior Researcher, Atomic Frequency Standards Group, Applied Research and Standards Division*

*Frequency Standard, Laser Spectroscopy*



**HASEGAWA Atsushi, Ph. D.**

*Senior Researcher, Quantum Information Technology Group, Basic and Advanced Research Division*

*Non-linear Laser Spectroscopy*



**ITO Hiroyuki, Ph. D.**

*Researcher, Atomic Frequency Standards Group, Applied Research and Standards Division*

*Atomic Frequency Standards*



**KUMAGAI Motohiro, Ph. D.**

*Researcher, Atomic Frequency Standards Group, Applied Research and Standards Division*

*Atomic Standard, Laser Physics*



**KOTAKE Noboru**

*Researcher, Japan Standard Time Group, Applied Research and Standards Division*

*Time and Frequency Standard*



**KAJITA Masatoshi, Dr. Sci.**

*Senior Researcher, Atomic Frequency Standards Group, Applied Research and Standards Division*

*Quantum Electronics, Atom & Molecular Physics*



**HOSOKAWA Mizuhiko, Ph. D.**

*Leader, Atomic Frequency Standards Group, Applied Research and Standards Division*

*Atomic Frequency Standards, Space Time Measurements*



**MORIKAWA Takao**

*Research Supervisor, Applied Research and Standards Division*

